Glutaredoxin-1 up-regulation induces soluble vascular endothelial growth factor receptor 1, attenuating post-ischemia limb revascularization

Colin E. Murdoch[1,2], Michaela Shuler[1,2], Dagmar J.F. Haeussler[1,2], Priyanka Bearelly[1,2], Ryosuke Kikuchi[2], Jingyan Han[1,2], Yosuke Watanabe[1,2], José J. Fuster[2], Kenneth Walsh[2], Ye-Shih Ho[3], Markus M. Bachschmid[1,2], Richard A. Cohen[1,2], and Reiko Matsui[1,2 *]

[1]Vascular Biology Section, [2]Whitaker Cardiovascular Institute, Department of Medicine, Boston University, Boston MA 02118.

[3]Institute of Environmental Health Science, Department of Biochemistry and Molecular Biology, Wayne State University, Detroit MI 48202.

Running Title: Anti-angiogenic soluble Flt induction by glutaredoxin-1

*Correspondence to: Reiko Matsui, MD. Vascular Biology Section, Department of Medicine, Boston University, 650 Albany Street, Boston, Massachusetts 02118, USA. Phone: 617-638-7114, Fax: 617-638-7113, E-mail: rmatsui@bu.edu

Key Words: animal models, angiogenesis, glutathionylation, ischemia, NF-kB, redox regulation, VEGF.

Capsule

Background: Glutaredoxin-1 (Glrx) inhibits endothelial cell migration by reversing protein-glutathione adducts.

Results: Revascularization after hind-limb ischemia was inhibited in Glrx transgenic mice. Glrx overexpression increased soluble VEGF receptor 1 (sFlt) in endothelial cells via NF-kB-dependent Wnt5a production.

Conclusion: Glrx enhances Wnt5a-induced anti-angiogenic sFlt in endothelial cells.

Significance: Up-regulated Glrx inhibits VEGF signaling by increased sFlt causing impaired vascularization.

Abstract

Glutaredoxin-1 (Glrx) is a cytosolic enzyme that regulates diverse cellular function by removal of GSH adducts from *S*-glutathionylated proteins including signaling molecules and transcription factors. Glrx is up-regulated during inflammation and diabetes. Glrx overexpression inhibits VEGF-induced endothelial cell (EC) migration. The aim was to investigate the role of up-regulated Glrx in EC angiogenic capacities and *in vivo* revascularization in the setting of hind limb ischemia. Glrx overexpressing EC from Glrx transgenic mice (TG) showed impaired migration and network formation and secreted higher level of soluble VEGF receptor 1 (sFlt), an antagonizing factor to VEGF. After hind limb ischemia surgery Glrx TG mice demonstrated impaired blood flow recovery, associated with lower capillary density and poorer limb motor function compared to wild type littermates. There were also higher levels of anti-angiogenic sFlt expression in the muscle and plasma of Glrx TG mice after surgery. Non-canonical Wnt5a is known to induce sFlt. Wnt5a was highly expressed in ischemic muscles and EC from Glrx TG mice, and exogenous Wnt5a induced sFlt expression and inhibited network formation in human microvascular EC. Adenoviral Glrx-induced sFlt in EC was inhibited by a competitive Wnt5a inhibitor. Furthermore, Glrx overexpression removed GSH adducts on p65 in ischemic muscle and EC, and enhanced nuclear factor kappa B (NF-kB) activity which was responsible for Wnt5a-sFlt induction. Taken together, up-regulated Glrx induces sFlt in EC via NF-kB -dependent Wnt5a, resulting in attenuated revascularization in hind limb ischemia. The Glrx-induced sFlt may be a part of mechanism of redox regulated VEGF signaling.

Introduction

Excess levels of reactive oxygen and nitrogen species (RONS) contribute to various pathological conditions. However, physiological levels of RONS are also essential for cellular signaling in part through modification of redox sensitive cysteine thiols on proteins. Exposure of reactive cysteine thiols to RONS in the presence of glutathione (GSH) results in *S*-glutathionylation, a reversible post-translational modification. GSH adducts may provide signaling mechanism and protect proteins from irreversible oxidation during fluctuations of RONS levels (1). This reversible modification can result in functional inhibition (2–4) or activation (5, 6) of a broad range of proteins with redox-sensitive thiols. Thus, regulation of GSH adducts has significance in various clinical conditions (7). Glutaredoxin-1 (Glrx) is a cytosolic enzyme that specifically catalyzes the removal of GSH adducts from *S*-glutathionylated proteins (P-SSG) (8). Therefore, Glrx can regulate cellular functions including signal transduction, cytoskeleton dynamics, and gene transcription by reversing *S*-glutathionylation (9, 10). A well-studied example is the NF-kB pathway wherein GSH adducts inactivate inhibitor of kappa B kinase (IKK) β [3] and inhibit DNA binding of p50 (11) and p65 (12) subunits, thus Glrx promotes NF-kB activation by removing GSH adducts (7, 13, 14). Glrx expression is increased in atherosclerotic human coronary artery (15), allergic mouse airway (16), and diabetic rat retina (13). Plasma Glrx activity is increased in type 2 diabetic patients (17), suggesting an association with oxidative stress. However, because GSH adducts have various effects on protein function, the cellular effects of increased Glrx are more

complex than that of an antioxidant enzyme, and may differ depending on tissue and pathological conditions.

Vascular endothelial growth factor A (VEGF) is a major factor to stimulate arteriogenesis and angiogenesis. VEGF binds VEGF receptor 2 (VEGFR2; Kdr/Flk1) resulting in receptor dimerization and phosphorylation of tyrosine residues. VEGFR2 is the main transducer of VEGF on endothelial proliferation, migration, and network formation (18). However, VEGF binds to VEGFR1 (fms-like tyrosine kinase-1; Flt) with higher affinity than VEGFR2. Flt can function as a negative regulator for VEGFR2 since a full-length membrane-tethered Flt (mFlt) transduces a weaker signal than VEGFR2, and a soluble splice variant (sFlt) can capture the VEGF ligand as a decoy to prevent its binding to VEGFR2 (18, 19). A number of redox-sensitive proteins are involved in VEGF signaling (20). *S*-glutathionylation inactivates protein tyrosine phosphatases (4, 21) and thus promotes tyrosine phosphorylation of VEGF receptor and signaling.

We previously observed that Glrx overexpression inhibited endothelial angiogenic properties *in vitro* (22). In contrast, a report suggests Glrx overexpression may be beneficial for recover of cardiac dysfunction after ischemia (23). Therefore, we dissected the mechanism in which Glrx inhibits EC migration and examined whether Glrx up-regulation *in vivo* may improve or inhibit post-ischemic revascularization using Glrx overexpressing mice. The overexpression of Glrx was similar to the increase in enzyme activity observed in the onset of diseases such as diabetes.

As a result, we found that Glrx overexpressing EC produced higher level of anti-angiogenic sFlt, and inhibiting sFlt expression reversed the anti-angiogenic effects of Glrx in EC. *In vivo*, the blood flow recovery after femoral artery ligation was significantly impaired in association with poorer motor function in Glrx transgenic (TG) mice compared to WT mice. Interestingly, plasma levels of the inhibitory VEGF receptor sFlt were higher in the Glrx TG mice. Accordingly, we found that Glrx overexpression up-regulated non-canonical Wnt ligand, Wnt5a (wingless-type MMTV integration site family, member 5A) in ischemic muscle and cultured endothelial cells. Wnt5a in myeloid cells was shown to inhibit post-natal angiogenesis through Flt induction (24). Wnt5a activates NF-kB via β-catenin-independent signaling in endothelial cells (25), while inflammatory stimuli induce Wnt5a via NF-kB activation in monocytes (26, 27). We showed that exogenous Wnt5a treatment increased sFlt expression in EC and inhibited endothelial network formation. Our data indicate that Wnt5a regulates sFlt in endothelial cells in an autocrine/paracrine fashion, and Glrx up-regulation enhanced the Wnt5a-sFlt pathway, in part through NF-kB activation, and resulted in inhibition of *in vivo* revascularization in hind-limb ischemia.

MATERIALS AND METHODS

Mouse Hind limb ischemia (HLI) model—Animal study protocols were approved by the Institutional Animal Care and Use Committee at Boston University. Glrx TG mice were generated with Human Glrx overexpression driven by the human β-actin promoter at the laboratory of Dr. YS. Ho (Wayne State University, Detroit) (23). Heterozygote Glrx TG mice and wild-type (WT) littermates, male 8-9 month old, were subjected to unilateral HLI by surgical excising left femoral artery and vein as previously described (28, 29).

Blood flow measurements and the functional scores—Blood flow perfusion was measured by LASER Doppler (Moor Instruments UK) on plantar aspects of the feet of anesthetized mice (ketamine (100mg/kg) xylazine (10mg/kg); i.p.) as previously described (28). Severity of the ischemia was scored by assessment of limb function and mobility. Using the following criteria under blinded conditions; 1. No use of limb, 2. No use of foot, 3. Dragging of foot, 4. No toe spreading, 5. Full use of foot. Limb function of all mice was scored at the same time as blood flow measurements prior to sedation. Functional agility was measured on day 10 post-surgery by running on a treadmill until exhaustion.

Histological assessment—Capillary density was quantified in non-ischemic and ischemic gastrocnemius muscle by histological assessment, by isolectin B4 (Vector labs) staining.

ELISA—Murine VEGF-A and soluble VEGFR1 ELISA (R&D Systems) were performed on plasma from WT and Glrx TG mice and media collected from endothelial cells.

Aortic sprouting assay—Aortic rings from WT and Glrx TG mice were placed on growth factor-reduced Matrigel (BD Bioscience) supplemented with DMEM, 2% FBS and 1% penicillin/ streptomycin. Experiments were conducted using 4 mice from each group and 4-5 rings per mouse and area of outgrowth was measured using ImageJ.

Isolation of mouse endothelial cells—Microvascular ECs were selectively (CD31, BD Pharmagin) isolated from heart from WT and Glrx TG mice using a Macs Automated Cell Sorter (Miltenyi Biotec) after digestion in gentleMACS^{TM} Dissociator (Miltenyi Biotec).

Endothelial cell network formation—Quiescent ECs were seeded ($1x10^4$ cells /well) in 96-well plates coated with Matrigel (growth factor reduced; BD Biosciences). Network formation was assessed after treatment with or without VEGF (50ng/ml) in low serum endothelial growth media (Lonza) (22). Network formation was scored or length measured in a blinded manner as previously described (30).

Endothelial proliferation—Quiescent ECs were seeded ($1x10^4$ cells /well) in gelatin coated 96-well plates. After 24 hours EC proliferation was measured in the presence and absence of VEGF (50ng/ml) in EBM2 media with 0.5% FBS using cell proliferation kit (Biovision).

Endothelial cell migration—As previously described (30), EC migration was measured in the presence and absence of VEGF (50ng/ml) after performing scratch in a confluent monolayer of WT and TG mECs. Migration was quantified at four defined locations by measuring the area of the scratch per well at 0 and 18h using ImageJ.

Glutaredoxin activity assay—Glrx activity in muscle homogenate was determined by the NADPH dependent reduction of 2-hydroxyethildisulfide (HED) (31).

Glrx adenoviral overexpression—Adenovirus expressing human Glrx was a generous gift from Dr. Young J. Lee (University of Pittsburgh) (32) and it has been used in previous reports (22, 33). Human cardiac microvascular endothelial cells (hEC, Lonza) were infected in FBS-free EBM2 media with Glrx or β-galactosidase (LacZ) (control) adenoviruses with 10 μg/ml Polybrene™ (Sigma) and subsequently used for 72 hours.

siRNA in hECs—After adenoviral overexpression of LacZ or Glrx, p65 knockdown was achieved using on-target plus siRNA (Dharmacon). hEC were transfected with siRNA against p65 (200 pmol; Dharmacon) or non-silencing control using Lipofectamine™ 2000 reagent (Invitrogen) following manufacturer instructions. Cells were used in experiments 48-72 hours after transfection. Specific knockdown of sFLT was achieved by targeting two siRNA sequences to the unique 3' sequence of sFLT (Dharmacon siGENOME) as previously reported (34).

qRT-PCR—Total RNA was isolated from tissues or cells using TRIzol™ reagent (Invitrogen) and cDNA generated utilizing High Capacity RNA-to-cDNA kit (Invitrogen). Quantitative PCR was conducted using inventory mouse (Mm) and human (Hs); gene-specific TaqMan™ primers (Life Technologies): Glrx (Mm00728386_m1), (Hs00829752_g1); Wnt5a (Mm00437347_m1), (Hs00998537_m1); mFLT (Mm00438980_m1); VEGFA (Mm01281449_m1), (Hs0090055_m1); Flk/KDR (Mm00440111_m1), (Hs00911700_m1); Ror2 (Mm00443470_m1); E-selectin (Hs00950401_m1); IL6 (Hs00985639_m1); β-actin; mouse (4352933), human (4326315). Expression was obtained and analyzed using comparative Ct ($\Delta\Delta C_T$) with StepOne™ Real Time PCR software (Applied Biosystems), normalized to β-actin. The sequence for the custom designed TaqMan™ assay to assess human sFlt transcript was kindly provided by Dr. Stefanie Dimmeler (35). SYBR green primers were used to assess murine mFlt and sFlt according to the transcripts as published (24).

NF-kB luciferase activity assay—NF-kB reporter activity in WT and Glrx TG mEC was assessed by co-transfection with pNF-kB-LUC reporter and Renilla luciferase adenoviruses. The EC were stimulated with TNFα (100ng/ml, Sigma) for 4h and subsequent dual luciferase for *Firefly* luciferase and Renilla luciferase (Promega) activity was measured using a Tecan luminometer. The NF-kB luciferase activity was normalized to the Renilla luciferase activity (NF-kB/Renilla luciferase activity).

Hypoxia—Endothelial cells in EBM2 with 0.1% FBS were incubated at 0.5% or 0.1% O_2, 70% humidity at 37ºC in a hypoxia chamber (Pathology Devices, Inc.) for 20 hours prior to isolation for biotin switch assay.

Biotin switch assay—*S*-glutathionylation of p65 was assessed as previously described (30, 36), hECs were lysed with maleimide (100mol/L) to block free cysteines. Modified thiols were reduced with DTT (20mM) and subsequently labeled with biotin-HPDP (N-[6-(biotinamido) hexyl]-3'-(2'-pyridyldithio) propionamide) (Peirce). Biotinylated proteins were purified with magnetic streptavidin agarose beads (Pierce) and biotin-HPDP modified proteins were immunoblotted with anti-p65 antibody (Cell Signaling).

Reagents—Reagents were obtained as follows; Recombinant Wnt5a (RD systems), Wnt5a antagonist Box5 (Millipore), rat-anti-Wnt5a antibody (RD systems). Human and mouse Glrx antibodies were custom ordered by Bethyl Laboratories, Inc.

Statistical Analysis—All group data are reported as mean ± SEM except as otherwise indicated. For the experimental data, statistical analysis comparing two groups was carried out using Student's unpaired t-test. Analysis of more than two groups was performed either by One-way ANOVA or Two-way ANOVA followed by Tukey post-hoc comparison test. Sequential measurements were analyzed by repeated measure one-way ANOVA. Analyses were completed using GraphPad Prism v5.0. *P values <0.05* were considered significant.

RESULTS

VEGF-induced migration and network formation diminished in Glrx TG endothelial cells—To understand the functional significance of endothelial Glrx on angiogenic function, we explored the function of Glrx overexpressing endothelial cell *in vitro* and *ex vivo*. Microvascular endothelial cells ($Cd31^+$) were selectively isolated from WT and Glrx TG hearts. Human Glrx expression was confirmed in Glrx TG mouse microvascular endothelial cells (mEC), and there was no change in endogenous Glrx expression between WT and Glrx TG mECs (Figure 1A). Furthermore, we assessed mEC network formation and migration. VEGF-induced network formation of mEC seeded on Matrigel was significantly inhibited in Glrx TG compared to WT mEC (Figure 1B&C). VEGF-induced migration was also attenuated in Glrx TG mEC (Figure 1D&E). In addition, mouse aorta rings were cultured *ex vivo* on Matrigel to assess endothelial sprouting. VEGF (50 ng/ml)-induced sprouting was attenuated in Glrx TG aortae compared to WT (Figure 1F&G). Together these data indicate VEGF-induced angiogenic function was impaired in Glrx TG derived endothelial cells.

Soluble Flt isoform was induced by Glrx overexpression—Alternative splicing of the anti-angiogenic Flt gene results in the membrane anchored isoform (mFlt) and a soluble isoform that is secreted extracellularly (sFlt). In seeking a mechanism for decreased angiogenic behavior of Glrx TG EC, we used primers specific for different Flt isoforms and found both sFlt and mFlt mRNA expression were increased in mEC isolated from Glrx TG mice compared to cells from WT control (Figure 2A&B). Hypoxia induces sFLT expression in ECs. After 24 hours hypoxic treatment, sFlt and mFlt expression remained significantly higher in TG ECs. To determine if EC could secrete sFlt, we collected media (after 24h quiescence) from mEC isolated from Glrx TG and WT mice under normoxic and hypoxia conditions. sFlt levels were markedly greater in media from Glrx TG mEC compared to WT mEC. Interestingly a marked increase was observed with hypoxic treatment in TG mECs (Figure 2C).

Inhibiting sFlt reverses the anti-angiogenic effect of Glrx—In order to elucidate the contribution of sFlt in the anti-angiogenic role of Glrx, we specifically knocked-down sFlt in human ECs using siRNA designed to target the unique C-terminal region of the sFlt isoform as previously reported in human endothelial cells (34).

In order to be able to utilize the reported sFLT siRNA we used human microvascular endothelial cells (hEC) and induced Glrx overexpression by adenoviral infection. Glrx adenoviral overexpression in human EC (22) caused the same phenotype we observed in microvascular EC isolated from Glrx mice, *i.e.* inhibition of migration and network formation. Quantitative PCR showed significant suppression of sFlt mRNA with siRNA for sFlt (Figure 2D). Proliferation was decreased in ECs overexpressing Glrx, however knockdown of sFlt reinstated the level of proliferation observed in LacZ treated ECs (Figure 2E). Likewise, sFlt knockdown rescued Glrx-induced attenuation of EC migration (Figure 2F&G). Furthermore, EC network formation that

was inhibited by Glrx overexpression was reversed with sFlt knockdown (Figure 2H&I). Together these data confirm that Glrx inhibits endothelial function through sFlt.

Wnt5a is increased by Glrx overexpression and regulates sFlt in EC—It has recently been reported that Wnt5a inhibits developmental angiogenesis through Flt regulation in myeloid cells (24). Therefore, we investigated whether Glrx increased sFlt via Wnt5a induction. Wnt5a expression was increased in mECs isolated from Glrx TG mice (Figure 3A). In addition, receptor tyrosine kinase-like orphan receptor 2 (Ror2), a receptor for the Wnt5a ligand (37) was also up-regulated in Glrx TG mECs (Figure 3B). To explore the control of sFlt expression further, hEC were treated with recombinant Wnt5a. Wnt5a (100 ng/ml) induced a marked but transient increase in mRNA expression of sFlt and mFlt within 3 hrs (Figure 3C&D). Next, EC network formation and migration were evaluated in response to Wnt5a treatment. After 24 h incubation with Wnt5a, human endothelial network formation was inhibited (Figure 3E&F) similar to the observations in Glrx TG mEC. Interestingly, Glrx overexpression in hEC resulted in increased Wnt5a mRNA expression, which was associated with increased sFlt expression (Figure 3G&H). To determine the role of Wnt5a on the expression of sFlt in these cells, the Wnt5a competitive antagonist, Box5 was utilized to block non-canonical Wnt5a signalling (38). hEC infected with Glrx or LacZ were treated with or without Box5 (100μM, 18h). Box5 prevented Glrx-induced sFlt expression in hEC (Figure 3I). Together, our data indicate that Wnt5a increases sFlt in human endothelial cells as shown previously in myeloid cells (24) and confirm that Glrx induces sFlt via Wnt5a in EC.

Glrx overexpression impairs in vivo blood recovery after femoral artery ligation —To investigate the *in vivo* role of Glrx up-regulation on post-ischemia re-vascularization, Glrx TG mice were utilized in which overexpression of the human Glrx transgene was achieved by the β-actin promoter (Figure 4A). (27). Expression of the human Glrx observed in TG gastrocnemius muscle had no effect on endogenous Glrx expression as murine Glrx protein was similar between Glrx TG and WT mice (Figure 4B). The additional Glrx expression from transgene resulted in a significant 3-fold increase in Glrx activity in the TG muscle and heart homogenate compared with WT homogenate (Figure 4C) which was similar level of increase in Glrx activity observed in diabetic animals (13). Hind limb ischemic blood flow recovery was compared in Glrx TG mice to WT littermate controls. Blood flow was assessed serially after HLI surgery (day 0, 3, 7 and 14) by LASER Doppler speckle tracking in the plantar aspect of the paws (Figure 4E). In WT mice blood flow recovery was evident on day 3, whereas Glrx TG blood flow was consistently lower over the 2-week measurement period (Figure 4D&E, $P<0.05$, repeated measured ANOVA). Glrx TG mice often had a necrotic toes and feet (Figure 4F). The functional impact of impaired revascularization was assessed by examining ambulatory foot movement. Scoring of motor function showed Glrx TG mice were less able to use the ischemic limb, whereas WT mice generally had full use of the limb and their toes had grip reflex 7 days after the surgery (Figure 4G). To further examine the consequence of ischemia on limb motor function, mice were placed on a treadmill and exercise function was assessed by calculating the time required to run until exhaustion (akin to the clinical walk test conducted on peripheral artery disease patients). Ten days after surgery Glrx TG mice showed impairment of limb function as they ran for a shorter time period compared to WT mice (Figure 4H). As blood flow recovery in part corresponds to increased tissue capillary density, we examined the capillary density in gastrocnemius muscle. As expected, in WT mice, capillary density increased in the ischemic gastrocnemius muscle, however in the ischemic Glrx TG muscle there was a marked attenuation of the capillary increase (Figure 4I&J). There was no significant difference in capillary density in non-ischemic limbs.

Soluble Flt expression is increased in Glrx TG mouse muscle and plasma—In accordance with the increase in sFlt in Glrx overexpressing EC, we found both sFlt and mFlt mRNA expression were higher in Glrx TG ischemic muscle compared to WT control 14-days after HLI surgery (Figure 5A&B), whereas no difference was observed in VEGF and VEGFR2 expression (Figure 5C&D). Furthermore, the level of sFlt, assessed by ELISA was significantly higher in plasma from Glrx TG mice on both 4 and 14 days post-HLI (Figure 5E).

We analyzed VEGF levels in mouse plasma 4 and 14 days after the HLI surgery by ELISA and found no difference in circulating VEGF levels (Figure 5F). Interestingly, Wnt5a expression was markedly increased in Glrx TG ischemic muscle compared to WT. In contrast, Wnt5a levels were low in non-ischemic limb from both WT and Glrx TG mice (Figure 5G). These data suggest that Wnt5a and sFlt induction in Glrx overexpressing EC might occur in Glrx TG mice.

Glrx removes p65-NF-kB GSH adducts in ischemic muscle and EC—We used a biotin switch assay to quantify reversible cysteine modifications. This assay first irreversibly blocks free cysteines, and then selectively labels reversible cysteine modifications with biotin-HPDP after reduction with DTT. The HPDP modified proteins are then precipitated with streptavidin and blotted for the protein of interest to indicate the level of thiol modification of that protein. Interestingly, we found that thiol adducts on p65 were increased in the ischemic muscle of WT mice (Figure 6A&B), but were significantly attenuated in that of Glrx TG mice, consistent with a decrease in GSH adducts. This also indicates significantly higher Glrx activity (removing GSH adducts) *in vivo* in Glrx TG mice. Thus, confirming that the modest increase observed in Glrx activity (Figure 4C) has an *in vivo* biological consequence. We also found that adenoviral overexpression of Glrx lowered GSH adducts of p65 compared to LacZ infected EC (Figure 6C). Furthermore, Glrx overexpression prevented the increase in GSH adducts on p65 under hypoxia (0.1%, 20h) (Figure 6C&D).

Glrx enhances Wnt5a and sFlt in a NF-kB-dependent manner—To confirm that removal of glutathione adducts enhanced NF-kB activity in Glrx TG EC, an NF-kB-reporter assay was used in isolated mEC treated with TNFα, a well described NF-kB activator. TNFα stimulated greater NF-kB activity in Glrx TG mEC compared to WT mEC (Figure 7A). Next, we investigated whether the inhibition of NF-kB activity could prevent Glrx-induced Wnt5a expression. We used human ECs overexpressing Glrx by adenovirus infection. First, hEC were treated with MG132, a proteasome inhibitor, which stabilizes IκBα and inhibits NF-kB. MG132 prevented the transcriptional up-regulation of Wnt5a by Glrx overexpression (Figure 7B). Likewise, we assessed if siRNA knockdown of p65 could prevent Wnt5a expression. SiRNA treatment was effective after 72 hours, inhibiting p65 protein expression (Figure 7C), and preventing TNFα-induced E-selectin (Figure 7D) and AdGlrx induced IL-6 expression (Figure 7E) which validate p65 knockdown inactivating NF-kB. Furthermore, siRNA knockdown of p65 attenuated the AdGlrx-induced increase in Wnt5a and sFlt observed in hECs (Figure 7F&G). AdGlrx expression had no effect on VEGFR2 expression, whereas p65 knockdown increased VEGFR2 expression (Figure 7H). Together these data indicate that induction of Wnt5a expression by Glrx is mediated via NF-kB activation, and promotes sFlt production in EC, summarized in Figure 8.

DISCUSSION

Glutathione adducts on redox-sensitive cysteine thiols are becoming increasingly recognized as an important mechanism for cellular signaling (39). Glrx specifically reverses protein-bound glutathione adducts, thus acting as a signaling switch on a range of important proteins (7, 40). Up-regulated Glrx under oxidative stress (e.g. ischemia) might accelerate turnover of GSH adducts, thus promoting pathological signaling. Our data reports for the first time that Glrx regulates anti-angiogenic sFlt production through the non-canonical Wnt5a pathway that may have important implications in ischemic vascular disease, as up-regulation of Glrx impaired ischemic limb revascularization.

Up-regulated Glrx resulted in impaired ischemic limb revascularization and exercise function. In addition, capillary density in the ischemic muscle from Glrx mice was lower compared to WT mice. Interestingly, the alternative splice variant of VEGFR1 (Flt), sFlt was increased in plasma after HLI surgery from Glrx TG mice. In addition, we detected higher sFlt in the media of EC isolated from Glrx TG mice. VEGFR2 mainly transduces VEGF-induced angiogenic responses, while Flt negatively regulates angiogenic signals by sequestering VEGF with high affinity to prevent the ligand binding to VEGFR2, and the membrane-tethered Flt (mFlt) appears to have weaker tyrosine kinase activity than VEGFR2 in angiogenic signaling (18). Adenoviral sFlt gene transfer inhibited revascularization in murine HLI

(41). Elevated sFlt during pregnancy has been implicated in pre-eclampsia (42) and peripartum cardiomyopathy (43) by anti-angiogenic mechanisms. Soluble Flt expression was elevated in the serum of diabetic rats (44) and the ischemic muscle of diet-induced diabetic mice in association with impaired blood flow after femoral artery ligation (45). Glrx expression is associated with various disease processes. Glrx levels were shown to be higher in diabetic rat (13) and in plasma from diabetic patients (17). In this study we used mice that overexpressed Glrx to a similar degree to the pathological level (13). Our findings may help to explain why diabetic patients have poor revascularization capability and a higher incidence of vascular ischemia, intermittent claudication and lower limb amputations (45).

Soluble Flt production is regulated by alternatively splicing (35), and ectodomain shedding of Flt by proteolytic cleavage has also been suggested as a mechanism of sFlt production in cancer cells (46). Using primers which distinguish the splice variants, we found that Glrx overexpression increased mFlt as well as sFlt in human and mouse EC. At this point, it is not clear whether splicing factors and/or ectodomain shedding are regulated by Glrx. VEGF gene expression and VEGF levels in plasma were not different by Glrx TG, and VEGFR2 expression was not altered by Glrx overexpression in EC.

Previously, Stefater *et al.* reported that the non-canonical Wnt ligand, Wnt5a, in myeloid cells inhibited postnatal angiogenesis by inducing sFlt (24). The importance of Wnt ligands as developmental regulators of cell proliferation, migration, differentiation, and polarity are well known. In addition, recent reports suggest inhibitory roles of myeloid derived Wnt5a in developmental angiogenesis and wound repair (24, 47). Surprisingly, Wnt5a was highly expressed in ischemic hind limb muscle of Glrx TG compared to WT control. Also, Wnt5a expression was significantly higher in EC from Glrx TG mice, and Glrx overexpression increased Wnt5a as well as sFlt mRNA in human EC, suggesting that dysregulation of Wnt5a in the adult may have pathological significance. Recombinant Wnt5a induced sFlt in EC and inhibited EC network formation extending the previous finding in myeloid cells (24) to a different cell type. Ror2 is involved in non-canonical Wnt5a signaling and is a negative regulator of canonical Wnt/β-catenin pathway (37, 48). Elevation of Wnt5a levels causes increases in Ror2 expression (49). We found that Ror2 expression was significantly higher in Glrx TG derived EC consistent with Wnt5a responsiveness being increased in Glrx TG mice. Furthermore, competitive Wnt5a inhibitor, Box5, blocked Glrx-induced sFlt mRNA in EC, suggesting Glrx-induced sFlt in EC is Wnt5a-dependent.

Wnt5a causes p65 nuclear translocation and inflammation in EC (25), but also Wnt5a can be induced via NF-kB activation in monocytes (26, 27). As previously mentioned, Glrx promotes NF-kB activation through reversing *S*-glutathionylation of NF-kB components. We demonstrated higher TNFα-induced NF-kB activity in Glrx overexpressing EC. Moreover, using a biotin switch assay we showed Glrx decreased reversible thiol modifications on p65 in ischemic muscle and EC. Specific DNA binding of NF-kB (p50, p65) is inhibited by GSH adducts (11, 12, 23). We speculate IKKβ and p50 might be *S*-glutathionylated as well and contribute to NF-kB activation by Glrx, although we were unable to show that by the biotin switch method. Inhibition of NF-kB by MG132 or siRNA to p65 blocked Wnt5a induction by Glrx overexpression. In addition, Glrx-induced sFlt was attenuated in EC through NF-kB inhibition. These data indicate that Glrx induced Wnt5a and sFlt is related to activation of NF-kB. Glrx expression itself is induced by NF-kB activity (50) and up-regulated by inflammation and diabetes (13), suggesting deleterious positive feedback of the Glrx-NF-kB-Wnt5a pathway. In accordance with our data, inhibition of NF-kB with mutant IkBα increased disorganized vasculature in ischemic mouse hind limb (51) and enhanced tumor growth (52), suggesting tight regulation of NF-kB is required to maintain normal vascularization (53).

A recent report suggests that after coronary artery ligation, Glrx TG mice may have improved neovascularization and cardiac remodeling due to less apoptosis (23). In their report, they showed α-actin staining was increased in the heart and VEGF expression was elevated, which may be insufficient to conclude that Glrx TG promotes eovascularization in heart. Higher VEGF expression does not necessarily correlate with

angiogenesis (45). They also showed hyper-activation of NF-kB that may contribute the protection of myocytes from apoptosis. Glrx may be protective in ischemic heart due to inhibition of apoptosis. We conducted a more extensive study on angiogenic properties in Glrx overexpressing EC and mice. Our results clearly demonstrated that up-regulated Glrx inhibits EC migration and network formation *in vitro*, and impairs hindlimb revascularization *in vivo.*

In myeloid cells Wnt5a induction of sFlt is likely through nuclear factor of activated T cells (NFAT) activation (47). Interestingly, the interaction between NFAT and NF-kB p65 promotes synergistic activation of NFAT (54). Also, many transcription factors are known to be redox-sensitive including AP-1/c-Jun (55), p53 (56), Nrf-2 and its regulatory protein, Keap-1 (57). Therefore, other transcriptional regulation might be involved in Glrx-induced Wnt5a and sFlt. Furthermore, we assume there may be multiple Glrx targets involved in VEGF and angiogenesis signaling because many related proteins are known to be *S*-glutathionylated, such as SERCA (5), H-Ras (33, 36), PTP1B (4), β-actin (10, 58), eNOS (59), and sirtuin-1 (2), all of which could be involved. Further studies will elucidate redox-sensitive regulation of sFlt induction.

In summary, we report a novel pathway by which Glrx overexpression induces sFlt through increasing Wnt5a in EC, resulting in impaired *in vivo* revascularization after limb ischemia. In addition, we extended the importance of Wnt5a-sFlt pathway to endothelial cells. These results are of significant importance because Glrx is up-regulated in pathological conditions including diabetes in which ischemic conditions are worsened.

ACKNOWLEDGEMENTS

The authors thank Leah Mycoff and Pratibha Chauhan for technical assistance.

This work was supported, in whole or in part, by National Institutes of Health Grants PO1 HL 068758, R37 HL104017, and NHLBI contract number HHSN268201000031C (RAC), and HL081587 (KW). This work was also supported by Robert Dawson Evans Scholar Award to RAC from the Department of Medicine, Boston University School of Medicine.

Disclosures: The authors have no conflict of interest.

REFERENCES

1. Klatt, P., and Lamas, S. (2000) Regulation of protein function by S-glutathiolation in response to oxidative and nitrosative stress. *Eur. J. Biochem.* **267**, 4928–44

2. Zee, R. S., Yoo, C. B., Pimentel, D. R., Perlman, D. H., Burgoyne, J. R., Hou, X., McComb, M. E., Costello, C. E., Cohen, R. a, and Bachschmid, M. M. (2010) Redox regulation of sirtuin-1 by S-glutathiolation. *Antioxid. Redox Signal.* **13**, 1023–32

3. Reynaert, N. L., van der Vliet, A., Guala, A. S., McGovern, T., Hristova, M., Pantano, C., Heintz, N. H., Heim, J., Ho, Y.-S., Matthews, D. E., Wouters, E. F. M., and Janssen-Heininger, Y. M. W. (2006) Dynamic redox control of NF-kappaB through glutaredoxin-regulated S-glutathionylation of inhibitory kappaB kinase beta. *Proc. Natl. Acad. Sci. U. S. A.* **103**, 13086–91

4. Barrett, W. C., DeGnore, J. P., Keng, Y. F., Zhang, Z. Y., Yim, M. B., and Chock, P. B. (1999) Roles of superoxide radical anion in signal transduction mediated by reversible regulation of protein-tyrosine phosphatase 1B. *J. Biol. Chem.* **274**, 34543–6

5. Adachi, T., Weisbrod, R. M., Pimentel, D. R., Ying, J., Sharov, V. S., Schöneich, C., and Cohen, R. A. (2004) S-Glutathiolation by peroxynitrite activates SERCA during arterial relaxation by nitric oxide. *Nat. Med.* **10**, 1200–7

6. Clavreul, N., Bachschmid, M. M., Hou, X., Shi, C., Idrizovic, A., Ido, Y., Pimentel, D., and Cohen, R. A. (2006) S-glutathiolation of p21ras by peroxynitrite mediates endothelial insulin resistance caused by oxidized low-density lipoprotein. *Arterioscler. Thromb. Vasc. Biol.* **26**, 2454–61

7. Mieyal, J. J., Gallogly, M. M., Qanungo, S., Sabens, E. A., and Shelton, M. D. (2008) Molecular mechanisms and clinical implications of reversible protein S-glutathionylation. *Antioxid. Redox Signal.* **10**, 1941–88

8. Chrestensen, C. A., Starke, D. W., and Mieyal, J. J. (2000) Acute cadmium exposure inactivates thioltransferase (Glutaredoxin), inhibits intracellular reduction of protein-glutathionyl-mixed disulfides, and initiates apoptosis. *J. Biol. Chem.* **275**, 26556–65

9. Shelton, M. D., and Mieyal, J. J. (2008) Minireview Molecules and Regulation by Reversible S-Glutathionylation : Molecular Targets Implicated in Inflammatory Diseases. **25**, 332–346

10. Bachschmid, M. M., Xu, S., Maitland-Toolan, K. A., Ho, Y.-S., Cohen, R. A., and Matsui, R. (2010) Attenuated cardiovascular hypertrophy and oxidant generation in response to angiotensin II infusion in glutaredoxin-1 knockout mice. *Free Radic. Biol. Med.* **49**, 1221–9

11. Pineda-Molina, E., Klatt, P., Vázquez, J., Marina, a, García de Lacoba, M., Pérez-Sala, D., and Lamas, S. (2001) Glutathionylation of the p50 subunit of NF-kappaB: a mechanism for redox-induced inhibition of DNA binding. *Biochemistry* **40**, 14134–42

12. Qanungo, S., Starke, D. W., Pai, H. V, Mieyal, J. J., and Nieminen, A.-L. (2007) Glutathione supplementation potentiates hypoxic apoptosis by S-glutathionylation of p65-NFkappaB. *J. Biol. Chem.* **282**, 18427–36

13. Shelton, M. D., Kern, T. S., and Mieyal, J. J. (2007) Glutaredoxin regulates nuclear factor kappa-B and intercellular adhesion molecule in Müller cells: model of diabetic retinopathy. *J. Biol. Chem.* **282**, 12467–74

14. Shelton, M. D., Distler, A. M., Kern, T. S., and Mieyal, J. J. (2009) Glutaredoxin regulates autocrine and paracrine proinflammatory responses in retinal glial (muller) cells. *J. Biol. Chem.* **284**, 4760–6

15. Okuda, M., Inoue, N., Azumi, H., Seno, T., Sumi, Y., Hirata Ki, Kawashima, S., Hayashi, Y., Itoh, H., Yodoi, J., and Yokoyama, M. (2001) Expression of glutaredoxin in human coronary arteries: its potential role in antioxidant protection against atherosclerosis. *Arterioscler. Thromb. Vasc. Biol.* **21**, 1483–7

16. Reynaert, N. L., Wouters, E. F. M., and Janssen-Heininger, Y. M. W. (2007) Modulation of glutaredoxin-1 expression in a mouse model of allergic airway disease. *Am. J. Respir. Cell Mol. Biol.* **36**, 147–51

17. Du, Y., Zhang, H., Montano, S., Hegestam, J., Ekberg, N. R., Holmgren, A., Brismar, K., and Ungerstedt, J. S. (2013) Plasma glutaredoxin activity in healthy subjects and patients with abnormal glucose levels or overt type 2 diabetes. *Acta Diabetol.*

18. Koch, S., and Claesson-Welsh, L. (2012) Signal transduction by vascular endothelial growth factor receptors. *Cold Spring Harb. Perspect. Med.* **2**, a006502

19. Kendall, R. L., and Thomas, K. A. (1993) Inhibition of vascular endothelial cell growth factor activity by an endogenously encoded soluble receptor. *Proc. Natl. Acad. Sci. U. S. A.* **90**, 10705–9

20. Ushio-Fukai, M. (2006) Redox signaling in angiogenesis: role of NADPH oxidase. *Cardiovasc. Res.* **71**, 226–35

21. Abdelsaid, M. A., and El-Remessy, A. B. (2012) S-glutathionylation of LMW-PTP regulates VEGF-mediated FAK activation and endothelial cell migration. *J. Cell Sci.* **125**, 4751–60

22. Evangelista, A. M., Thompson, M. D., Weisbrod, R. M., Pimental, D. R., Tong, X., Bolotina, V. M., and Cohen, R. A. (2012) Redox regulation of SERCA2 is required for vascular endothelial growth factor-induced signaling and endothelial cell migration. *Antioxid. Redox Signal.* **17**, 1099–108

23. Adluri, R. S., Thirunavukkarasu, M., Zhan, L., Dunna, N. R., Akita, Y., Selvaraju, V., Otani, H., Sanchez, J. A., Ho, Y.-S., and Maulik, N. (2012) Glutaredoxin-1 overexpression enhances neovascularization and diminishes ventricular remodeling in chronic myocardial infarction. *PLoS One* **7**, e34790

24. Stefater, J. A., Lewkowich, I., Rao, S., Mariggi, G., Carpenter, A. C., Burr, A. R., Fan, J., Ajima, R., Molkentin, J. D., Williams, B. O., Wills-Karp, M., Pollard, J. W., Yamaguchi, T., Ferrara, N., Gerhardt, H., and Lang, R. A. (2011) Regulation of angiogenesis by a non-canonical Wnt-Flt1 pathway in myeloid cells. *Nature* **474**, 511–5

25. Kim, J., Kim, J., Kim, D. W., Ha, Y., Ihm, M. H., Kim, H., Song, K., and Lee, I. (2010) Wnt5a induces endothelial inflammation via beta-catenin-independent signaling. *J. Immunol.* **185**, 1274–82

26. Blumenthal, A., Ehlers, S., Lauber, J., Buer, J., Lange, C., Goldmann, T., Heine, H., Brandt, E., and Reiling, N. (2006) The Wingless homolog WNT5A and its receptor Frizzled-5 regulate inflammatory responses of human mononuclear cells induced by microbial stimulation. *Blood* **108**, 965–73

27. Nanbara, H., Wara-aswapati, N., Nagasawa, T., Yoshida, Y., Yashiro, R., Bando, Y., Kobayashi, H., Khongcharoensuk, J., Hormdee, D., Pitiphat, W., Boch, J. A., and Izumi, Y. (2012) Modulation of Wnt5a expression by periodontopathic bacteria. *PLoS One* **7**, e34434

28. Limbourg, A., Korff, T., Napp, L. C., Schaper, W., Drexler, H., and Limbourg, F. P. (2009) Evaluation of postnatal arteriogenesis and angiogenesis in a mouse model of hind-limb ischemia. *Nat. Protoc.* **4**, 1737–46

29. Ohashi, K., Ouchi, N., Higuchi, A., Shaw, R. J., and Walsh, K. (2010) LKB1 deficiency in Tie2-Cre-expressing cells impairs ischemia-induced angiogenesis. *J. Biol. Chem.* **285**, 22291–8

30. Haeussler, D. J., Pimentel, D. R., Hou, X., Burgoyne, J. R., Cohen, R. A., and Bachschmid, M. M. (2013) Endomembrane H-Ras Controls Vascular Endothelial Growth Factor-induced Nitric-oxide Synthase-mediated Endothelial Cell Migration. *J. Biol. Chem.* **288**, 15380–15389

31. Luthman, M., and Holmgren, A. (1982) Glutaredoxin from Calf Thymus. *J. Biol. Chem.* **257**, 6686–6690

32. Song, J. J., and Lee, Y. J. (2003) Differential role of glutaredoxin and thioredoxin in metabolic oxidative stress-induced activation of apoptosis signal-regulating kinase 1. *Biochem. J.* **373**, 845–53

33. Adachi, T., Pimentel, D. R., Heibeck, T., Hou, X., Lee, Y. J., Jiang, B., Ido, Y., and Cohen, R. A. (2004) S-glutathiolation of Ras mediates redox-sensitive signaling by angiotensin II in vascular smooth muscle cells. *J. Biol. Chem.* **279**, 29857–62

34. Ahmad, S., Hewett, P. W., Al-Ani, B., Sissaoui, S., Fujisawa, T., Cudmore, M. J., and Ahmed, A. (2011) Autocrine activity of soluble Flt-1 controls endothelial cell function and angiogenesis. *Vasc. Cell* **3**, 15

35. Boeckel, J.-N., Guarani, V., Koyanagi, M., Roexe, T., Lengeling, A., Schermuly, R. T., Gellert, P., Braun, T., Zeiher, A., and Dimmeler, S. (2011) Jumonji domain-containing protein 6 (Jmjd6) is required for angiogenic sprouting and regulates splicing of VEGF-receptor 1. *Proc. Natl. Acad. Sci. U. S. A.* **108**, 3276–81

36. Clavreul, N., Adachi, T., Pimental, D. R., Ido, Y., Schöneich, C., and Cohen, R. A. (2006) S-glutathiolation by peroxynitrite of p21ras at cysteine-118 mediates its direct activation and downstream signaling in endothelial cells. *FASEB J.* **20**, 518–20

37. Mikels, A., Minami, Y., and Nusse, R. (2009) Ror2 receptor requires tyrosine kinase activity to mediate Wnt5A signaling. *J. Biol. Chem.* **284**, 30167–76

38. Jenei, V., Sherwood, V., Howlin, J., Linnskog, R., Säfholm, A., Axelsson, L., and Andersson, T. (2009) A t-butyloxycarbonyl-modified Wnt5a-derived hexapeptide functions as a potent antagonist of Wnt5a-dependent melanoma cell invasion. *Proc. Natl. Acad. Sci. U. S. A.* **106**, 19473–8

39. Dulce, R. A., Schulman, I. H., and Hare, J. M. (2011) S-glutathionylation: a redox-sensitive switch participating in nitroso-redox balance. *Circ. Res.* **108**, 531–3

40. Fernandes, A. P., and Holmgren, A. (2004) Glutaredoxins: Glutathione-dependent redox enzymes with functions far beyond a simple thioredoxin backup system. *Antioxid. Redox Signal.* **6**, 63–74

41. Jacobi, J., Tam, B. Y. Y., Wu, G., Hoffman, J., Cooke, J. P., and Kuo, C. J. (2004) Adenoviral gene transfer with soluble vascular endothelial growth factor receptors impairs angiogenesis and perfusion in a murine model of hindlimb ischemia. *Circulation* **110**, 2424–9

42. Ahmad, S., and Ahmed, A. (2004) Elevated placental soluble vascular endothelial growth factor receptor-1 inhibits angiogenesis in preeclampsia. *Circ. Res.* **95**, 884–91

43. Patten, I. S., Rana, S., Shahul, S., Rowe, G. C., Jang, C., Liu, L., Hacker, M. R., Rhee, J. S., Mitchell, J., Mahmood, F., Hess, P., Farrell, C., Koulisis, N., Khankin, E. V, Burke, S. D., Tudorache, I., Bauersachs, J., del Monte, F., Hilfiker-Kleiner, D., Karumanchi, S. A., and Arany, Z. (2012) Cardiac angiogenic imbalance leads to peripartum cardiomyopathy. *Nature* **485**, 333–8

44. Khazaei, M., Fallahzadeh, A. R., Sharifi, M. R., Afsharmoghaddam, N., Javanmard, S. H., and Salehi, E. (2011) Effects of diabetes on myocardial capillary density and serum angiogenesis biomarkers in male rats. *Clinics* **66**, 1419–1424

45. Hazarika, S., Dokun, A. O., Li, Y., Popel, A. S., Kontos, C. D., and Annex, B. H. (2007) Impaired angiogenesis after hindlimb ischemia in type 2 diabetes mellitus: differential regulation of vascular endothelial growth factor receptor 1 and soluble vascular endothelial growth factor receptor 1. *Circ. Res.* **101**, 948–56

46. Rahimi, N., Golde, T. E., and Meyer, R. D. (2009) Identification of ligand-induced proteolytic cleavage and ectodomain shedding of VEGFR-1/FLT1 in leukemic cancer cells. *Cancer Res.* **69**, 2607–14

47. Stefater, J. A., Rao, S., Bezold, K., Aplin, A. C., Nicosia, R. F., Pollard, J. W., Ferrara, N., and Lang, R. A. (2013) Macrophage Wnt-Calcineurin-Flt1 signaling regulates mouse wound angiogenesis and repair. *Blood* **121**, 2574–8

48. Kikuchi, A., Yamamoto, H., Sato, A., and Matsumoto, S. (2012) Wnt5a: its signalling, functions and implication in diseases. *Acta Physiol. (Oxf).* **204**, 17–33

49. O'Connell, M. P., Fiori, J. L., Xu, M., Carter, A. D., Frank, B. P., Camilli, T. C., French, A. D., Dissanayake, S. K., Indig, F. E., Bernier, M., Taub, D. D., Hewitt, S. M., and Weeraratna, A. T. (2010) The orphan tyrosine kinase receptor, ROR2, mediates Wnt5A signaling in metastatic melanoma. *Oncogene* **29**, 34–44

50. Aesif, S. W., Kuipers, I., van der Velden, J., Tully, J. E., Guala, A. S., Anathy, V., Sheely, J. I., Reynaert, N. L., Wouters, E. F. M., van der Vliet, A., and Janssen-Heininger, Y. M. W. (2011) Activation of the glutaredoxin-1 gene by nuclear factor κB enhances signaling. *Free Radic. Biol. Med.* **51**, 1249–57

51. Tirziu, D., Jaba, I. M., Yu, P., Larrivée, B., Coon, B. G., Cristofaro, B., Zhuang, Z. W., Lanahan, A. a, Schwartz, M. a, Eichmann, A., and Simons, M. (2012) Endothelial nuclear factor-κB-dependent regulation of arteriogenesis and branching. *Circulation* **126**, 2589–600

52. Kisseleva, T., Song, L., Vorontchikhina, M., Feirt, N., Kitajewski, J., and Schindler, C. (2006) NF-κB regulation of endothelial cell function during LPS-induced toxemia and cancer. *J. Clin. Invest.* **116**, 2955–2963

53. Tabruyn, S. P., and Griffioen, A. W. (2007) A new role for NF-kappaB in angiogenesis inhibition. *Cell Death Differ.* **14**, 1393–7

54. Liu, Q., Chen, Y., Auger-Messier, M., and Molkentin, J. D. (2012) Interaction between NFκB and NFAT coordinates cardiac hypertrophy and pathological remodeling. *Circ. Res.* **110**, 1077–86

55. Klatt, P., Molina, E. P., and Lamas, S. (1999) Nitric oxide inhibits c-Jun DNA binding by specifically targeted S-glutathionylation. *J. Biol. Chem.* **274**, 15857–64

56. Velu, C. S., Niture, S. K., Doneanu, C. E., Pattabiraman, N., and Srivenugopal, K. S. (2007) Human p53 is inhibited by glutathionylation of cysteines present in the proximal DNA-binding domain during oxidative stress. *Biochemistry* **46**, 7765–80

57. Lukosz, M., Jakob, S., Büchner, N., Zschauer, T.-C., Altschmied, J., and Haendeler, J. (2010) Nuclear redox signaling. *Antioxid. Redox Signal.* **12**, 713–42

58. Wang, J., Boja, E. S., Tan, W., Tekle, E., Fales, H. M., English, S., Mieyal, J. J., and Chock, P. B. (2001) Reversible glutathionylation regulates actin polymerization in A431 cells. *J. Biol. Chem.* **276**, 47763–6

59. Chen, C.-A., Wang, T.-Y., Varadharaj, S., Reyes, L. A., Hemann, C., Talukder, M. A. H., Chen, Y.-R., Druhan, L. J., and Zweier, J. L. (2010) S-glutathionylation uncouples eNOS and regulates its cellular and vascular function. *Nature* **468**, 1115–8

Abbreviations and Acronyms used are: Glrx, glutaredoxin-1; EC, endothelial cells; mEC, cardiac mouse microvascular endothelial cells; hEC, human cardiac microvascular endothelial cells; HLI, hind limb ischemia; mFlt, membrane-bound VEGF receptor-1; RONS, reactive oxygen nitrogen species; Ror2, receptor tyrosine kinase-like orphan receptor 2; sFlt, soluble fms-like tyrosine kinase-1, VEGF receptor-1; VEGF, vascular endothelial growth factor A; Wnt5a, wingless-type MMTV integration site family, member 5A.

FIGURE LEGENDS

FIGURE 1. **Glrx overexpression attenuates EC-migration and network formation, as well as aortic sprouting.** A, Western blot analysis of human Glrx transgene or endogenous Glrx in WT and TG mouse microvascular ECs (mEC). B, Representative and C, quantitative blinded scoring of EC network formation in WT and TG mEC seeded onto Matrigel in the presence and absence of VEGF (50ng/ml) (n=6, * P<0.05). D, Representative and E, percentage wound closure of WT and TG mECs after 18h VEGF (50ng/ml) treatment, measured at 4-pre-determined locations (n=3, * P<0.05). F, Representative and G, quantitative assessment of sprouting of ECs from isolated WT and TG aortae after 6 days cultured on Matrigel in DMEM 2% FBS with and without VEGF (50ng/ml) (n=4, * P<0.05).

FIGURE 2. **Glrx attenuates EC function via the anti-angiogenic receptor, soluble FLT.** mRNA levels of A, sFlt and B, mFlt isoforms in WT and TG mouse microvascular endothelial cells (mEC) under normoxia and hypoxia (0.5% Oxygen, 20h, n=5, * P<0.05). C, ELISA; sFLT level in the media from WT and TG mEC in normoxic and hypoxic (0.5% Oxygen, 20h) conditions (n=5, * P<0.05, # P<0.01). D, sFlt mRNA expression by qPCR in human microvascular endothelial cells (hEC) treated with siRNA to sFlt (si-sFlt) or off-target scramble RNA (scr) after AdGlrx or AdLacZ infection (n=3, * P<0.05). E, Proliferation of hEC in the presence and absence of VEGF (50ng/ml, 24h) after adenoviral Glrx or LacZ overexpression and subsequent sFlt knockdown by siRNA compared to scr control (n=4, * P<0.05). F, Quantitative data and G, representative images of AdGlrx and AdLacZ treated hEC after 18h VEGF (50ng/ml) treatment, measured at 4-pre-determined locations. The effects of si-sFlt are shown compared to scr (n=5, * P<0.05). H, Quantitative measurement and I, representative images of EC network formation in AdGlrx and AdLacZ treated hEC with siRNA sFLT or scr control in the presence of VEGF (50ng/ml) (n=6, * P<0.05, *** P<0.001).

FIGURE 3: **Glrx causes a Wnt5a-dependent increase in sFLT expression in human ECs.** qRT-PCR analysis for A, Wnt5a and B, Ror2 mRNA in EC isolated from WT and TG mice (n=5, * P<0.05). qRT-PCR analysis of C, sFlt and D, mFlt in human microvascular endothelial cells (hEC) treated with rhWnt5a (100 ng/ml) over time indicated (n=5, * P<0.05). E, Representative images and F, quantitative assessment of hEC network formation in the presence and absence of Wnt5a (100 ng/ml, 24h), with and without VEGF treatment (50 ng/ml, 18h, n=4, * P<0.05). qRT-PCR for G, Wnt5a and H, sFlt in hECs overexpressing Glrx or LacZ by adenovirus treatment. (n=6, * P<0.05). I, sFlt mRNA expression in AdLacZ and AdGlrx treated hEC in the presence and absence of Box5 (Wnt5a antagonist, 100 µM, 24h. n=6, * P<0.05).

FIGURE 4: **Glrx overexpression attenuates revascularization, limb motor function, and capillary density after hind limb ischemia (HLI) surgery**. A, The structure of the human Glrx transgene driven by the β-actin promoter, CAP: transcriptional initiation site of the human β-actin gene. B, Western blot analysis of human Glrx transgene (hGlrx) and endogenous Glrx (mGlrx) in WT and TG gastrocnemius muscle. C, Glrx activity in heart and skeletal muscle homogenate from WT and Glrx TG mice. Activity was normalized to protein weight. (n=5. * =P<0.05). D, Quantitative serial assessment of LASER Doppler measuring blood flow recovery to the plantar aspect of WT and TG paws post hind-limb ischemia surgery (n=15, * P<0.05). E, representative LASER Doppler images obtained post-surgery and on day 14. F, representative images of ischemic paws from WT and TG mice 14 days after surgery. G, Scoring of motor function of ischemic limb from WT and TG mice on day 14 (n=12, * P<0.05). H, Duration of time on treadmill 10 days post-HLI surgery running at 5 m/min with 5 m/min increments every 5 minutes (n=6, * P<0.05). I, Representative images (scale 100µm) and J, quantitative analysis of isolectin B4 staining for capillaries in non-ischemic (NI) and ischemic (ISC) gastrocnemius muscle in WT and TG mice 14-days post-HLI surgery (n=5, * P<0.05).

FIGURE 5: **Up-regulation of the anti-angiogenic receptor, soluble FLT and Wnt5a in Glrx overexpressing mice post HLI.** mRNA expression of A, soluble and B, membrane bound Flt isoforms, C, VEGF and D, VEGFR2 in non-ischemic (NI) and ischemic (ISC) gastrocnemius muscles from WT and Glrx TG mice 14 days post-HLI (n=6, P<0.05). ELISA for E, sFLT1 and F, VEGF in plasma from WT and Glrx TG mice at 4 days (n=6) and 14 days (n=12) post-HLI (* P<0.05). G, Representative immunoblot of Wnt5a in non- and ischemic gastrocnemius muscle normalized to tubulin.

FIGURE 6. **Glrx decreases p65-glutathione adducts in ischemic muscle and endothelial cells**. A-D, Biotin switch assay showing the biotin labeled S-glutathionylated cysteines within p65 (pull down) in A, WT and Glrx TG non-ischemic (NI) and ischemic (ISC) muscle 4-days post-HLI, and in C, hEC overexpressing Glrx or LacZ under normoxic or hypoxic (0.1% 24h) conditions with (B&D) respective quantification of glutathione adducts normalized to p65-input, samples prior to incubation with streptavidin beads (n=3-4, * P<0.05, ** P<0.01).

FIGURE 7. **Glrx enhances Wnt5a and sFLT in a NF-kB-dependent manner.** A, NF-kB activity measured by luciferase reporter assay in the presence and absence of TNFα (50 ng/ml, 4h). NF-kB-reporter activity normalized to the co-transfected renilla-luciferase reporter in WT and Glrx TG mEC (* P<0.05, *** P<0.001; n=3). B, Wnt5a mRNA expression in AdGlrx infected hEC incubated with and without MG132 (1 μM, 24h; P<0.05, n=4). C-G, siRNA knockdown of p65 NFκB subunit on Glrx overexpressing hEC. C, Immunoblot for p65 and β-actin of hEC treated with a concentration range (10, 25, 50, 100nM, 72h) of siRNA to p65 or equivalent off-target control (scr). D, hEC mRNA for E-selectin after p65 knockdown (25nM) in the presence and absence of TNFα (40ng/ml) stimulation. E, IL-6, F, Wnt5a, G, sFlt, and H, VEGFR2 mRNA expression assessed by qRT-PCR after p65-siRNA or scrambled control treatment in AdGlrx or AdLacZ infected hEC (P<0.05, n=6).

FIGURE 8. **Elevated Wnt5a expression promotes sFlt induction in the Glrx up-regulated EC.** Summary of data in this study is shown. Glrx overexpression increased Wnt5a and sFlt mRNA and secretion of sFlt from EC, thus VEGF-induced vascularization is impaired. NF-kB inactivation (siRNA) suppressed Glrx-induced sFlt and Wnt5a. Wnt5a antagonist (BOX5) inhibited Glrx-induced sFlt. Exogenous Wnt5a increased sFlt in EC. Inhibiting sFlt (siRNA) improved angiogenic phenotype of EC overexpressing Glrx.

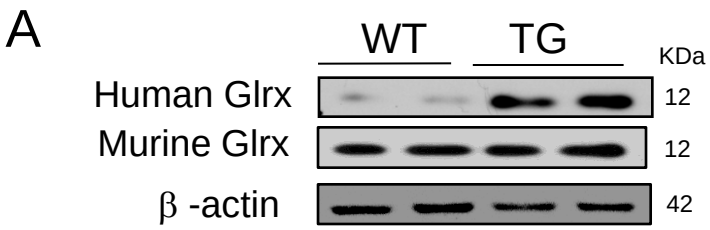
A
WT
TG
KDa
Human Glrx
Murine Glrx
β -actin
12
12
42

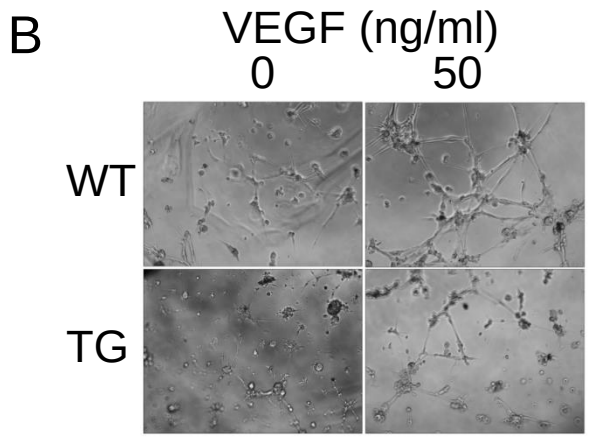
B
VEGF (ng/ml)
0
50
WT
TG

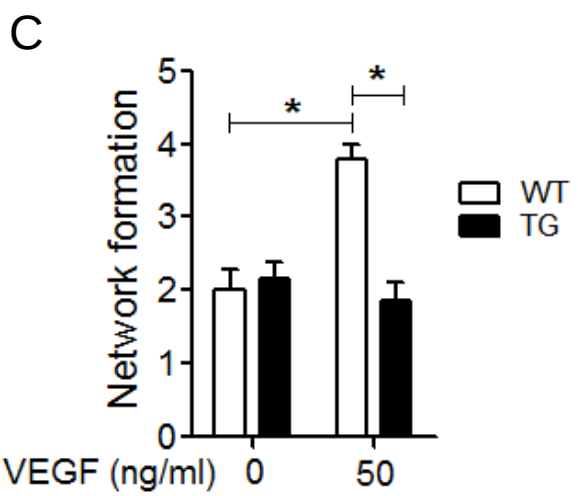
C
Network formation
5
4
3
2
1
0
*
*
WT
TG
VEGF (ng/ml) 0 50

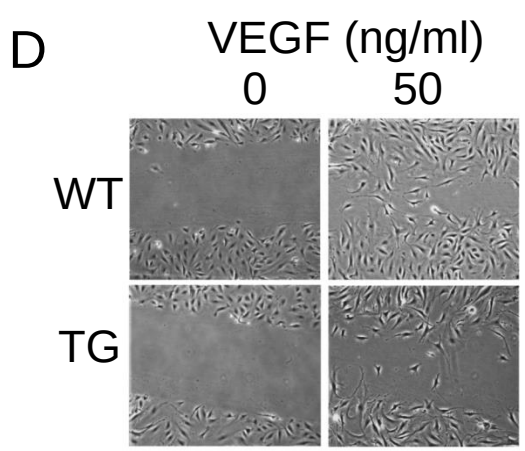
D
VEGF (ng/ml)
0
50
WT
TG

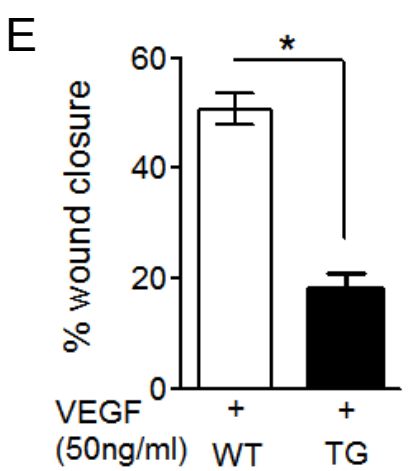
E
% wound closure
60
40
20
0
*
VEGF
(50ng/ml)
+
+
WT
TG

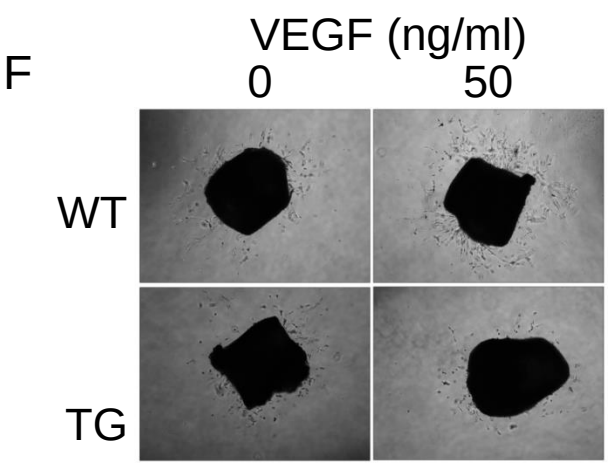
F
VEGF (ng/ml)
0
50
WT
TG

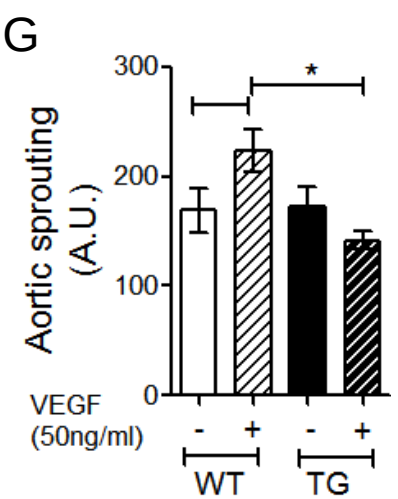
G
Aortic sprouting
(A.U.)
300
200
100
0
*
VEGF
(50ng/ml)
-
+
-
+
WT
TG

Figure 1

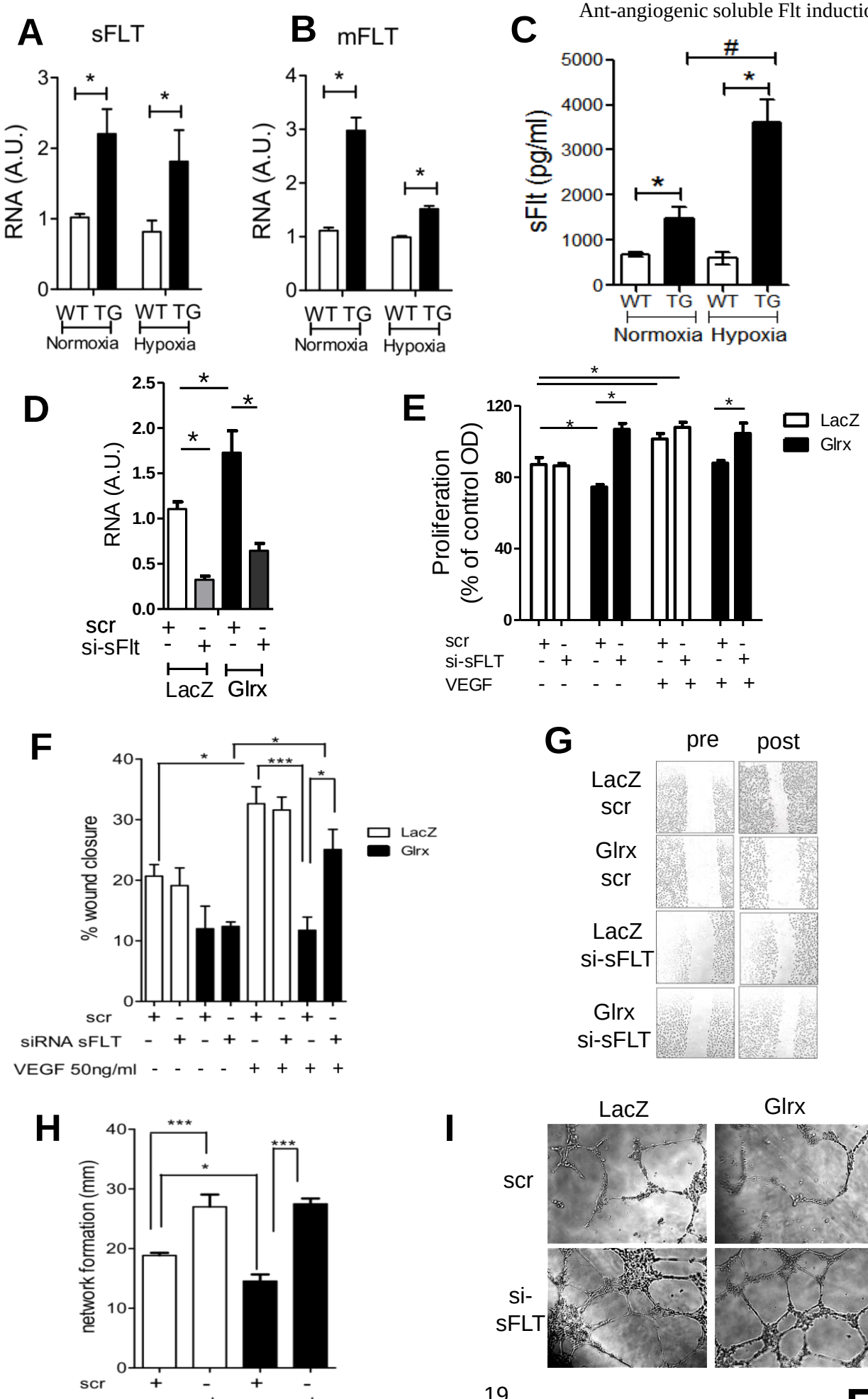
A
sFLT
RNA (A.U.)
WT TG WT TG
Normoxia Hypoxia
B
mFLT
RNA (A.U.)
WT TG WT TG
Normoxia Hypoxia
C
sFlt (pg/ml)
WT TG WT TG
Normoxia Hypoxia
D
RNA (A.U.)
scr
si-sFlt
LacZ Glrx
E
Proliferation (% of control OD)
LacZ
Glrx
scr
si-sFLT
VEGF
F
% wound closure
LacZ
Glrx
scr
siRNA sFLT
VEGF 50ng/ml
G
pre
post
LacZ scr
Glrx scr
LacZ si-sFLT
Glrx si-sFLT
H
network formation (mm)
scr
siRNA sFLT
LacZ Glrx
I
LacZ
Glrx
scr
si-sFLT

Figure 2

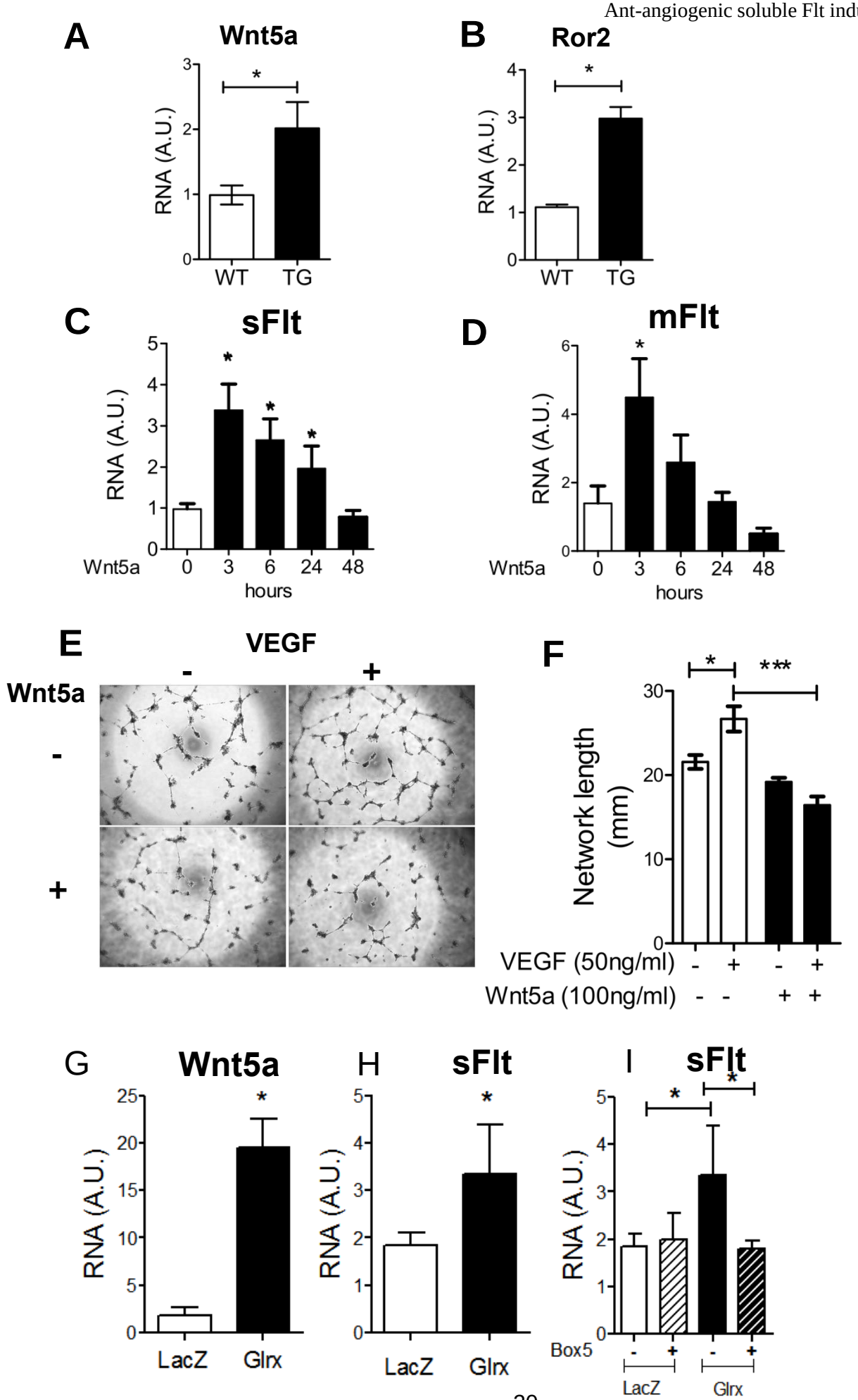
A
Wnt5a
RNA (A.U.)
WT
TG
B
Ror2
C
sFlt
Wnt5a
hours
D
mFlt
E
VEGF
Wnt5a
F
Network length (mm)
VEGF (50ng/ml)
Wnt5a (100ng/ml)
G
Wnt5a
LacZ
Glrx
H
sFlt
I
sFlt
Box5

Figure 3

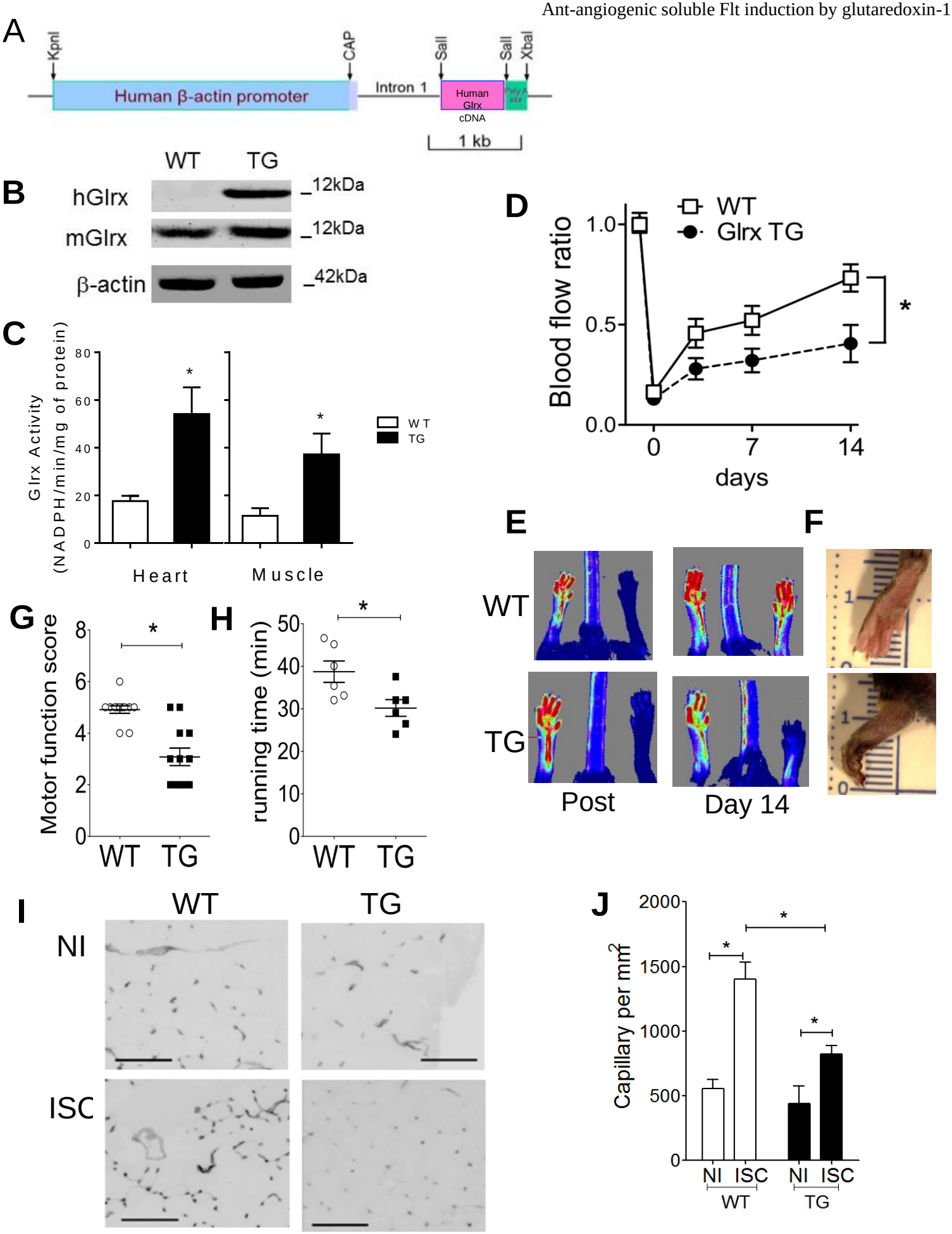
A
KpnI
CAP
SalI
SalI
XbaI
Human β-actin promoter
Intron 1
Human Glrx cDNA
Poly A site
1 kb
B
WT
TG
hGlrx
mGlrx
β-actin
12kDa
12kDa
42kDa
C
Glrx Activity (NADPH/min/mg of protein)
80
60
40
20
0
WT
TG
Heart
Muscle
D
Blood flow ratio
1.0
0.5
0.0
WT
Glrx TG
0
7
14
days
E
F
WT
TG
Post
Day 14
G
Motor function score
8
6
4
2
0
WT
TG
H
running time (min)
50
40
30
20
10
0
WT
TG
I
WT
TG
NI
ISC
J
Capillary per mm2
2000
1500
1000
500
0
NI
ISC
NI
ISC
WT
TG

Figure 4

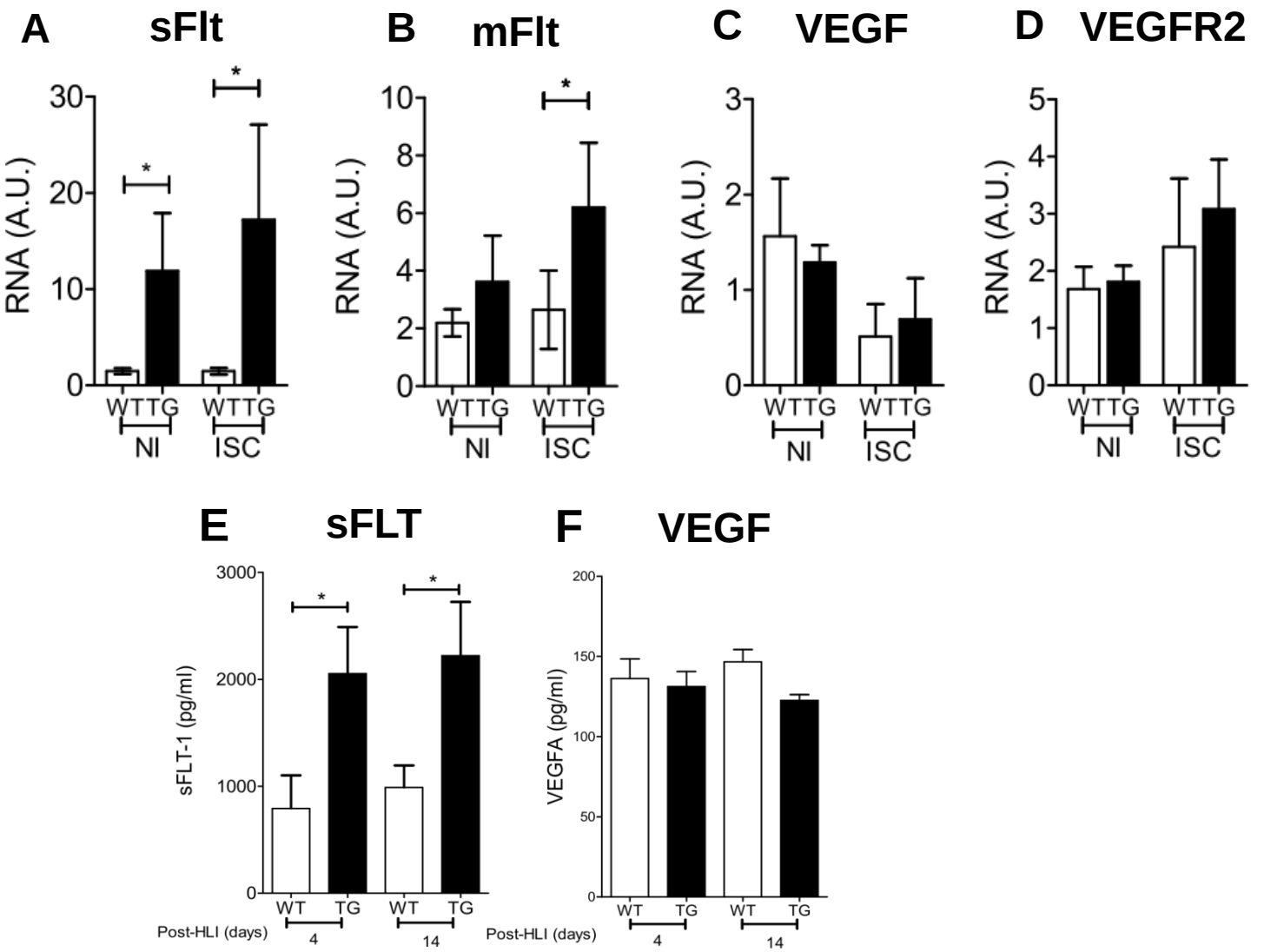
A
sFlt
B
mFlt
C
VEGF
D
VEGFR2
RNA (A.U.)
WT TG WT TG
NI ISC
E
sFLT
F
VEGF
sFLT-1 (pg/ml)
VEGFA (pg/ml)
Post-HLI (days)
4
14
G
Non-ischemic
Ischemic
WT
GlrxTG
Wnt-5a
Tubulin

Figure 5

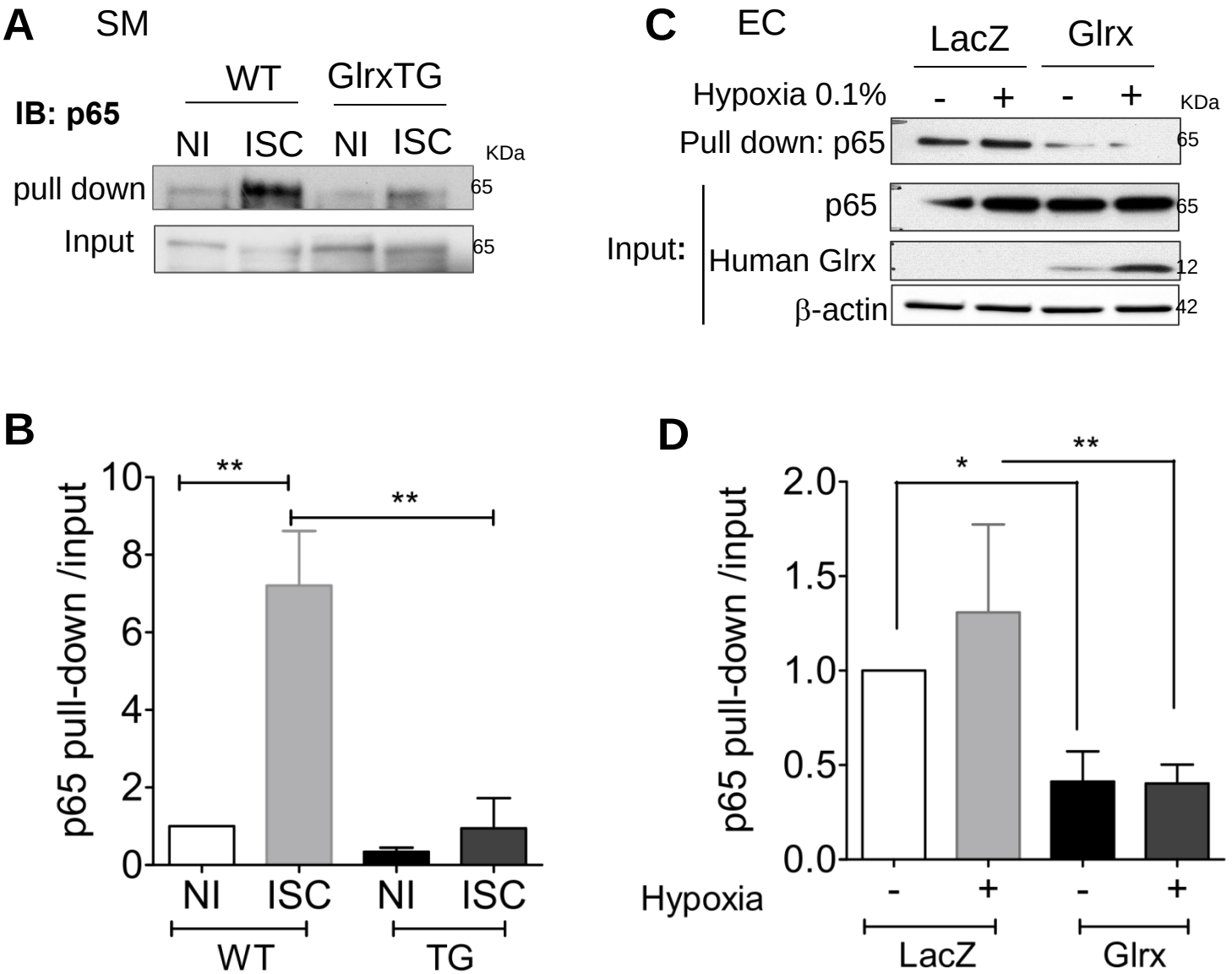
A
SM
WT
GlrxTG
IB: p65
NI
ISC
NI
ISC
KDa
pull down
65
Input
65
C
EC
LacZ
Glrx
Hypoxia 0.1%
-
+
-
+
KDa
Pull down: p65
65
Input:
p65
65
Human Glrx
12
β-actin
42
B
p65 pull-down /input
10
8
6
4
2
0
**
**
NI
ISC
NI
ISC
WT
TG
D
p65 pull-down /input
2.0
1.5
1.0
0.5
0.0
*
**
Hypoxia
-
+
-
+
LacZ
Glrx

Figure 6

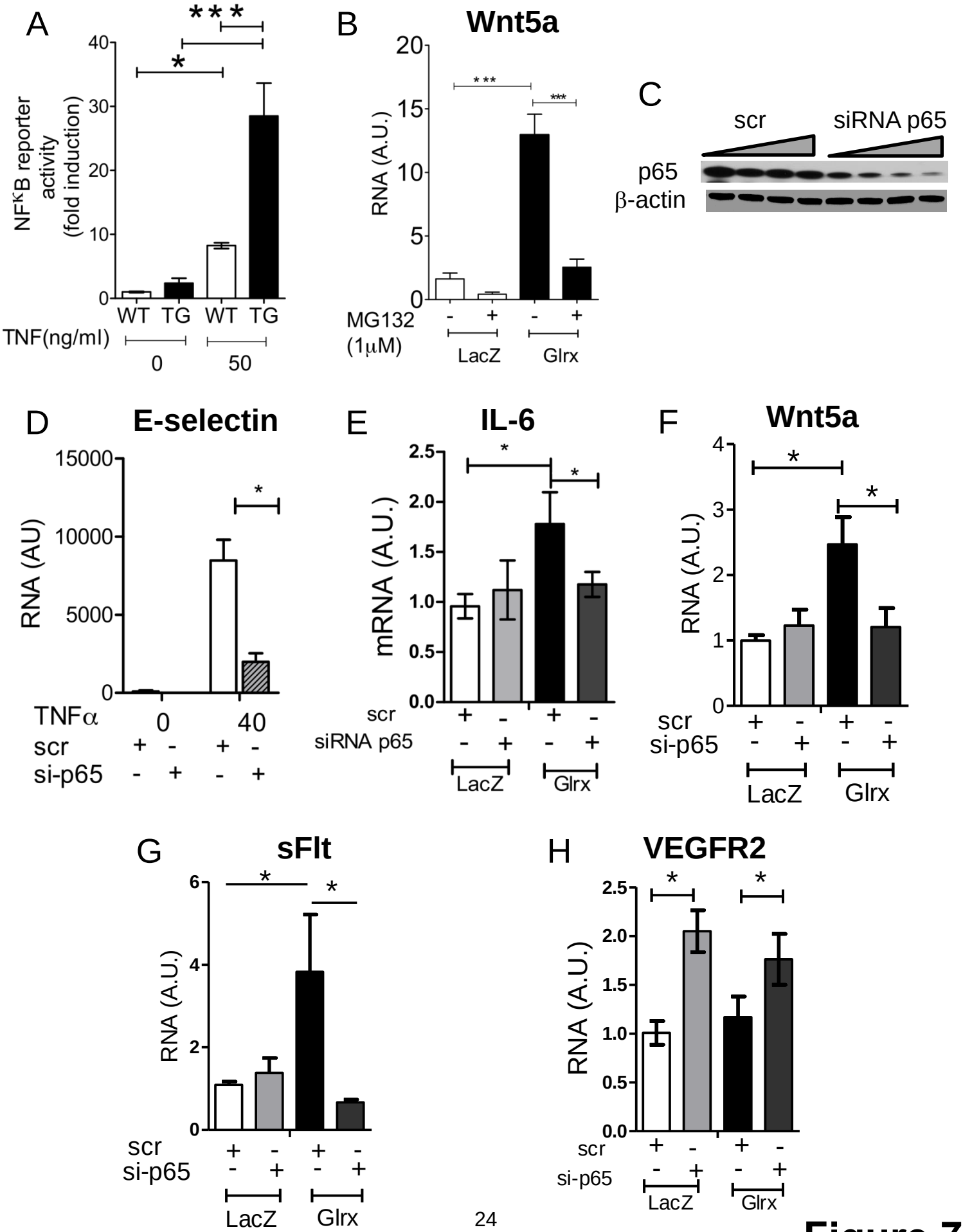
A
NFκB reporter activity (fold induction)
WT TG WT TG
TNF(ng/ml)
0 50
B
Wnt5a
RNA (A.U.)
MG132 (1μM)
LacZ Glrx
C
scr siRNA p65
p65
β-actin
D
E-selectin
RNA (AU)
TNFα 0 40
scr
si-p65
E
IL-6
mRNA (A.U.)
scr
siRNA p65
LacZ Glrx
F
Wnt5a
RNA (A.U.)
scr
si-p65
LacZ Glrx
G
sFlt
RNA (A.U.)
scr
si-p65
LacZ Glrx
H
VEGFR2
RNA (A.U.)
scr
si-p65
LacZ Glrx

Figure 7

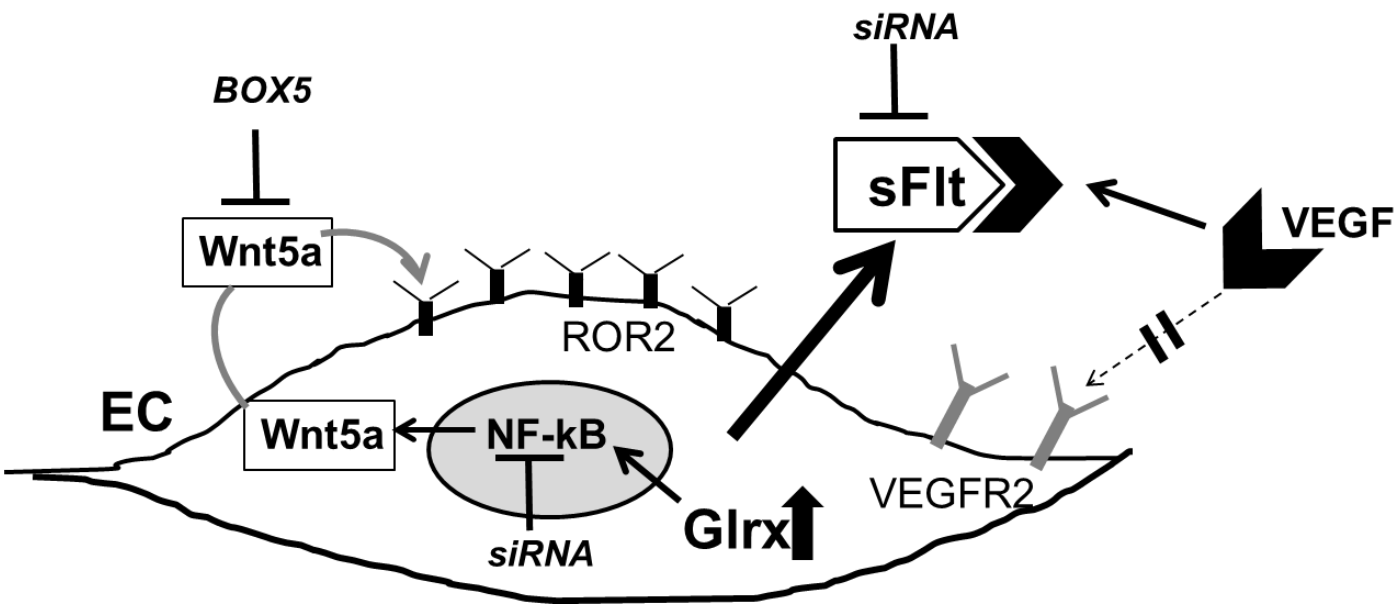
siRNA
BOX5
sFlt
VEGF
Wnt5a
ROR2
EC
Wnt5a
NF-kB
VEGFR2
siRNA
Glrx

Figure 8.